THE ASTROPHYSICAL JOURNAL, 608:L41–L44, 2004 June 10

THE POLYMERIZATION OF ACETYLENE, HYDROGEN CYANIDE, AND CARBON CHAINS IN THE NEUTRAL LAYERS OF CARBON-RICH PROTO–PLANETARY NEBULAE

JOSÉ CERNICHARO
Departamento de Astrofísica Molecular e Infrarroja, Instituto de Estructura de la Materia, CSIC, Serrano 121, E-28006 Madrid, Spain; cerni@damir.iem.csic.es
Received 2002 July 13; accepted 2004 April 26; published 2004 May 12

ABSTRACT

I present chemical evolution models for the neutral layers of proto–planetary nebulae in order to explain the high abundance of polyynes, cyanopolyynes, methyl-polyynes, benzene, and other C-bearing species found in CRL 618 by Cernicharo et al. In the neutral regions behind the H II region, the radiation field produces a rich photochemistry on timescales shorter than the dynamical evolution of the central H II region, leading to the formation of large carbon-rich molecules C_nH_2, $HC_{(2n+1)}N$, and C_n. Reactions between radicals H and H_2 play a crucial role in maintaining a high abundance for these species in spite of the strong radiation field emerging from the central star. The models predict that proto–planetary nebulae in the early stages of evolution will have high abundances for species such as $HC_{(2n+1)}N$, C_nH_4, and C_nH_3N. The role of reactions between neutrals and radicals in the growth of aromatic molecules is discussed. The large abundance derived for small cumulenes suggests that the growth of small carbon grains with $C/H \gg 1$ could be dominated by reactions between polyynes and cumulenes. The models also explain the observed abundances of H_2CO, OH, H_2O, CO_2, and [O I] in the region where CO is photodissociated.

Subject headings: astrochemistry — molecular data — molecular processes — planetary nebulae: individual (CRL 618) — stars: AGB and post-AGB

On-line material: color figure

1. INTRODUCTION

IRC +10216 is the prototype carbon-rich asymptotic giant branch (AGB) circumstellar envelope (CSE). The millimeter spectral survey of Cernicharo et al. (2000) indicates that the most abundant species are carbon-chain polyynic radicals (C_nH). Its infrared spectrum is dominated by CO, C_2H_2, and HCN (Cernicharo et al. 1996, 1999), and the observations with the *Infrared Space Observatory* (*ISO*) show no evidence of the unidentified infrared bands in this object. However, when C-rich stars evolve toward the planetary nebula phase (proto–planetary nebulae; PPNs), the UV photons ionize the CSE and produce a qualitative change in the chemistry in its neutral layers; rather than carbon chain radicals, the infrared spectrum of these objects shows large abundances of polyynes (C_nH_2), cyanopolyynes, benzene (C_6H_6), and methyl-polyynes (Cernicharo et al. 2001a, 2001b). Moreover, H_2CO, H_2O, OH, and atomic oxygen have been found in CRL 618 (Cernicharo et al. 1989; Herpin & Cernicharo 2000), and CO_2 has been detected in the Red Rectangle (Waters et al. 1998). Hence, the physical processes associated with this crucial phase of star evolution lead to the formation of aromatic molecules, long polyynes and cyanopolyynes, and O-bearing species. In this Letter, I present chemical models that explain the qualitative evolution of a dense and warm gas subjected to a strong photodissociating, but not ionizing, UV field. The models suggest that carbon clusters with $C/H \gg 1$ are formed in the neutral layers, the photodissociation region (PDR) precursor (PDRP), prior to the arrival of the ionizing field.

2. CHEMICAL MODELS

The physical structure of the CSE of CRL 618 is highly complex (Herpin & Cernicharo 2000). The strong UV field from the central star has produced an ultracompact H II region that is confined by a dense circumstellar disk (the "torus"). UV photons escape in the perpendicular direction with respect to the torus plane and illuminate the CSE, producing an extended PDR. However, the bulk of the HC_3N and HC_5N emission in the millimeter domain, and the absorption of C_2H_2, C_4H_2, C_6H_2, and benzene, arise from a region much smaller, the innermost region of the torus surrounding the central H II region. The goal of this work is to design a qualitative scheme for the chemical structure of the PDRP, and I have assumed three neutral layers (zones) of gas with different visual absorption. In the H II ultracompact region, the averaged electronic density is $\simeq 10^7$ cm^{-3} (Martin-Pintado et al. 1988), and I have assumed that all ionizing photons are absorbed in the PDR. Kwok & Bignell (1984) measured a size of $0''.1 \times 0''.4$ (2.5×10^{15}–10^{16} cm^2 for a distance of 1600 pc) for the H II region. They suggested that the termination of the mass-loss process of the AGB phase occured $\simeq$100 years ago, which means an expansion rate for the minor axis of the H II region of 2.5×10^{13} cm yr^{-1}. As the H II region is dusty (it occupies the highest density region of the CSE), the radiation field reaching the PDR is reduced by dust absorption. I will assume that at the PDRP the enhancement of the radiation field G with respect to the UV galatic field is 10^4. Zone I is the first neutral region of the PDRP and has a radial A_V of 1 mag. Its distance to the central star is 2.5×10^{15} cm and is subjected to a nonionizing radiation field with $G = 10{,}000$ (*ISO* data show very weak emission of [C II], mainly arising from the H II region; Herpin & Cernicharo 2000). Carbon monoxide and all molecular species are efficiently photodissociated in this zone. Zone II has $A_V = 2$ mag, and H_2 is well protected by zone I and by self-shielding. Atomic oxygen is available in these zones from the photodissociation of CO. In zone III, $A_V = 3$ mag, and H_2 and CO will be well protected against photodissociation. A temperature of 300 K and a density of 10^7 cm^{-3} has been assumed for zones I, II, and III (Cernicharo et al. 2001a, 2001b). The corresponding thickness of each layer is 1×10^{14} cm. Chemistry begins in the models by the photodissociation of the most abundant molecules: H_2, CO, C_2H_2, HCN, C_2H_4, and CH_4. The initial abundances

relative to H_2 adopted in zones I, II, and III are $x(CO) = 1.15 \times 10^{-3}$, $x(C_2H_2) = 5 \times 10^{-4}$, $x(CH_4) = 2 \times 10^{-4}$, $x(C_2H_4) = 10^{-4}$, and $x(HCN) = 10^{-4}$, which corresponds to a C/O ratio of $\simeq 3$ (Cernicharo et al. 2001a, 2001b). These values are not typical of the AGB phase, where depletion on the grains could reduce the abundance of some of these species but are only 2–5 times larger than those observed in IRC +10216 (Cernicharo et al. 1996, 1999).

The neutral-neutral reactions included in the models are all neutral bimolecular reactions, A + B = C + D in the UMIST database (Le Teuff et al. 1999), the chemical models of Titan and Saturn (Toublanc et al. 1995; Lara et al. 1996; Moses et al. 2000a, 2000b), and those found in low-pressure combustion and pyrolysis models (see, e.g., Konnov 2000; Kiefer et al. 1992; only reactions with measured rates at 300 K have been included from these databases). Missing possible important reactions (H, H_2+radicals) are discussed below. All rates have been revised following the last available data (NIST Chemical Kinetics Database, ver. 2Q98). In the following, all bimolecular reaction rates have units of $cm^{-3}\ s^{-1}$. The reactions of atomic and diatomic carbon with hydrocarbons are very fast and have been included in the models (Haider & Hussain 1993; Herbst et al. 1994; Herbst 2001; Chastaing et al. 2000, 2001; Millar et al. 2000, Kaiser et al. 2001, and references therein). Of particular interest are reactions R7 and R8, which lead to the growth of C_nH chains with n odd, and to high yield for C_3 (Clary et al. 2002, and references therein). Reaction between carbon chains $C_nH + C_mH_2$ up to $n + m = 16$ have been included in the model. Photodissociation rates for these species have been taken from the databases quoted above when available, or are assumed to be 10^{-10} otherwise. Photodissociation products for the cumulene chains C_n are assumed to be C_3 and C_{n-3} (Choi et al. 2000). The main set of reactions is shown in Table 1. Reverse rates have been derived from the thermodynamic properties of the molecules included in the model. The set of differential equations representing the chemical evolution of zones I, II, and III was solved using a standard routine for stiff problems, and the code has been checked against published results.

The reaction of molecular and atomic hydrogen with carbon radicals is an important issue in modeling the chemistry at high temperatures (R14). The reaction H_2+C_2H has been studied at different temperatures in the laboratory, with $k_{300} = 4.7 \pm 1.5 \times 10^{-13}$ (Peeters et al. 2002, and references therein). The same rate has been assumed for reactions R14 (see, e.g., Kiefer et al. 1992; Moses et al. 2000a, 2000b; Toublanc et al. 1995). At low temperature the reaction is very slow ($k_{100} \simeq 10^{-15}$) so these reactions will have little effect on the chemistry. The reaction between C_2 ($^1\Sigma_g^+$) and molecular hydrogen will control the abundance of C_2. The measured rate at $T = 300$ K is 1.4×10^{-12} (Pitts et al. 1982). On the other hand, $C_2(A^3\,\Pi_u)$ does react much more slowly with molecular hydrogen (Pitts et al. 1982). No data are available for the reaction of H_2 with longer cumulenes, except for C_3, for which an upper limit of $3 \times 10^{-14}\ cm^3\ s^{-1}$ has been obtained by Reisler et al. (1980). The adopted rate k_{300} for R13 is 10^{-14}. A rate of $k_{300} = 5.3 \times 10^{-13}$ has been adopted for R19 (the same value as for R18, which was obtained by a fit to all experimental data)

TABLE 1
MAIN REACTIONS INCLUDED IN THE MODEL

ID	Reaction	A ($cm^3\ s^{-1}$)	n	E (K)
R1	$C_nH + C_mH_2 = C_{n+m}H_2 + H$	2.7×10^{-10}	−0.43	0
R2	$C_2H + C_mH_2 = C_mH + C_2H_2$	3.3×10^{-11}	0.00	0
R3	$C_nH + C_mH = C_{n+m}H + H$	3.3×10^{-11}	0.00	0
R4	$C_nH + C_mH = C_nH_2 + C_m$	3.0×10^{-12}	0.00	0
R5	$C_2H + C_2H_4 = C_4H_4 + H$	2.0×10^{-11}	0.00	0
R6	$C + C_2H = C_3 + H$	3.3×10^{-10}	0.00	0
R7	$C + C_2H_2 = C_3H + H$	2.0×10^{-10}	0.00	0
R8	$C + C_2H_2 = C_3 + H_2$	2.0×10^{-10}	0.00	0
R9	$C + C_nH_m = C_{n+1}H_{m-1} + H$	3.3×10^{-10}	0.00	0
R10	$C_n + C_mH = C_{m+n} + H$	2.0×10^{-10}	0.00	0
R11	$H_2 + C = CH + H$	3.1×10^{-10}	0.16	11890
R12	$H_2 + C_2 = C_2H + H$	1.8×10^{-10}	0.00	1469
R13	$H_2 + C_n (n > 2) = C_nH + H$	1.0×10^{-14}	0.00	0
R14	$H_2 + C_nH = C_nH_2 + H$ $(n > 2)$	4.2×10^{-12}	1.67	624
R15	$H_2 + CH = H + CH_2$	2.7×10^{-10}	0.00	1545
R16	$H_2 + CH_2 = H + CH_3$	5.2×10^{-11}	0.17	6400
R17	$H_2 + CH_3 = H + CH_4$	2.0×10^{-14}	2.84	3864
R18	$H_2 + CN = HCN + H$	1.6×10^{-12}	2.06	1334
R19	$H_2 + C_nN = HC_nN + H$ $(n > 1)$	5.3×10^{-13}	0.00	0
R20	$H + CH = C + H_2$	1.3×10^{-10}	0.00	80
R21	$H + CH_2 = CH + H_2$	5.2×10^{-11}	0.00	−675
R22	$H + CH_3 = CH_2 + H_2$	1.0×10^{-10}	0.00	7600
R23	$H + CH_4 = CH_3 + H_2$	3.5×10^{-13}	3.11	3970
R24	$H + C_2H = C_2 + H_2$	8.4×10^{-11}	0.00	14330
R25	$CN + C_2H_4 = HCN + C_2H_3$	2.1×10^{-10}	0.00	0
R26	$CN + C_2H_4 = CH_2CHCN + H$	5.1×10^{-11}	−0.70	31
R27	$C_nN + C_mH_2 = HC_{n+m}N + H$	2.0×10^{-10}	0.00	0
R28	$O + CH_3 = H_2CO + H$	1.4×10^{-10}	0.00	0
R29	$O + C_2H_3 = OH + C_2H_2$	2.0×10^{-11}	0.00	0
R30	$CO + OH = CO_2 + H$	1.2×10^{-13}	0.95	−75
R31	$H_2 + OH = H_2O + H$	8.4×10^{-13}	0.00	1040

NOTE.—For this table, $k = A(T/300)^n e^{-(E/T)}$ and $T_K > 300$ K.

3. RESULTS

Figure 1 shows that very high abundances are predicted for polyynes, cyanopolyynes, and cumulene clusters. Most species reach peak abundances in $\simeq 0.2$ yr. Steady state (SS) in zones II and III is reached for most species in a few years. In zone II the ratio of the peak abundance to the SS abundance for polynnes, cumulenes, and cyanopolyynes is 10, 1, and 500, respectively. However, in zone III these values are of the order of unity. The abundance ratio $x(C_nH_2)/x(C_nH)$, $n > 2$, has peak and SS values of 100 and 20, respectively. However, the abundance ratio $x(C_2H_2)/x(C_2H)$ has a peak and SS value of 8 and 2, respectively. This is due to the reaction C_2+H_2 (R12), while the corresponding reaction for larger C_n (R13) is much slower. Reactions R14–R19 compete with photodissociation and preserve a high abundance for polyynes and cyanopolyynes and for the products of their reactions with other species. The photochemical polymerization of acetylene leads to the transformation of 99% of the initial C_2H_2 into longer polyyne and cumulene chains in zone II, and of $\simeq$90% in zone III. The abundance ratio between consecutive polyynes is 2–3 at $t =$ 1 yr, and close to unity after a few years when SS is reached. The chemical time to reach peak abundances is well below the expansion time of the H II region ($\simeq$4 yr, see above). Hence, when the ionization front reaches zone II and III, most acetylene has already been processed into longer, complex species. The polymerization of HCN is also very efficient, and HC_3N reaches an abundance similar to that of HCN. HC_5N will be 10 and 5 times less abundant than HC_3N in zones II and III, respectively. In zone I, all species will be photodissociated in $\simeq$2 yr. However, in absence of reactions R14–R19, the time to photodissociate the molecular gas will be 2 orders of magnitude shorter in this zone.

This long life for C_nH_2 species in zones II and III allows reactions with the most abundant radicals—C_2H, CN, and sev-

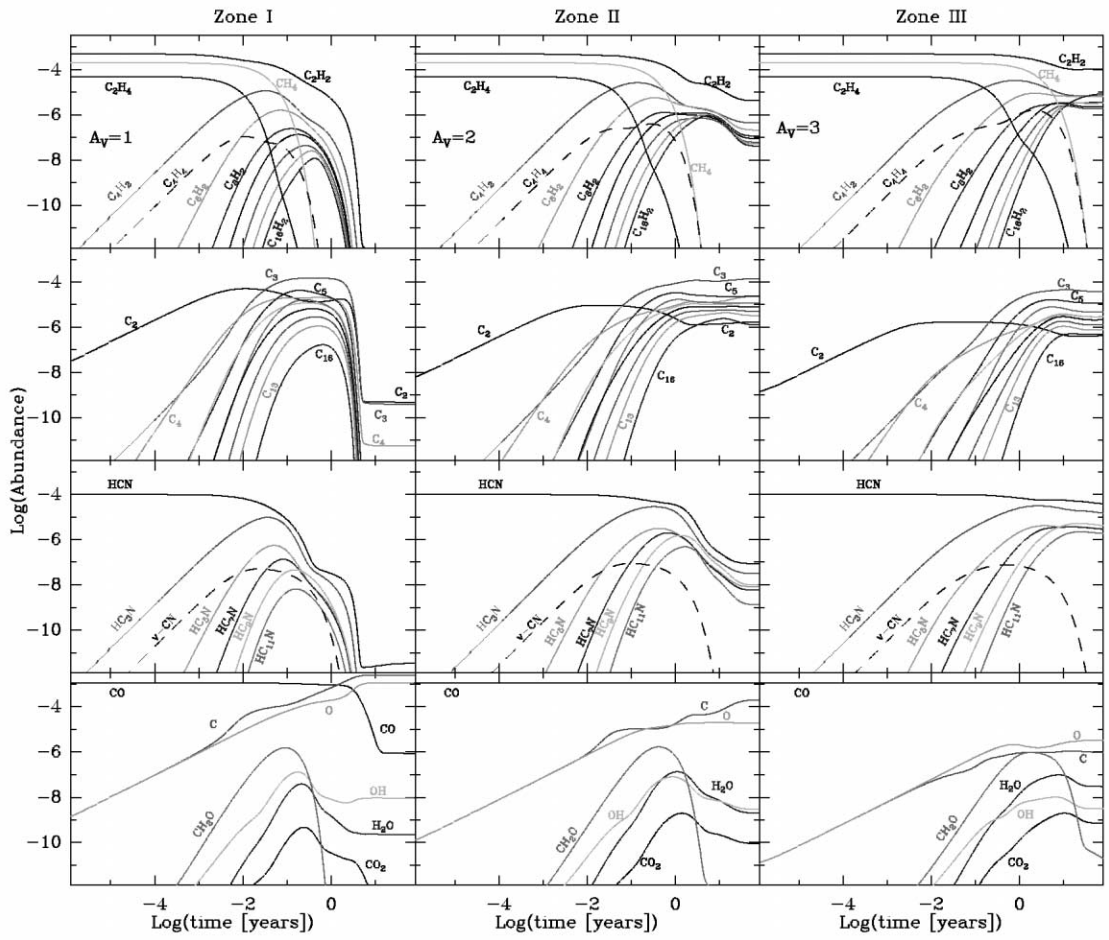

FIG. 1.—Molecular abundances in zones I, II, and III (*left to right*). Top panels show the abundance of polyynes, C_nH_2, CH_4, and C_2H_4. The abundance of vinyl-acetylene, C_4H_4, is shown as a dashed line. In zone I, full photodissociation of polyynes is slowed down by 2–3 orders of magnitude due to R14. The next row of panels shows the abundances of cumulenes C_n. Cyanopolyynes and vinyl-cyanide (dashed line labeled v-CN) are shown in the next row of panels. Finally, bottom panels show the abundance of O-bearing species and of atomic carbon and oxygen. Abundances are relative to the total gas density [$n(H) + 2n(H_2)$]. [*See the electronic edition of the Journal for a color version of this figure*.]

eral small carbon clusters—leading to the formation of long species. For densities as low as a few 10^5 cm^{-3}, the radicals C_nH become as abundant as the saturated species C_nH_2, and for lower densities they are more abundant (see the case of the external layer of IRC +10216). The millimeter spectral survey of CRL 618 (see Cernicharo et al. 2001a) shows relatively high abundances for the radicals, but with rotational temperatures much lower than those observed for C_nH_2 and HC_nN. They are produced in the external layers of CRL 618, while in the PDRP, polyynes and cyanopolyynes are much more abundant.

The photochemical polymerization of C_2H_2, and the low rate of the reaction of C_n with H_2, lead to very large abundances for the linear and cyclic cumulene chains. Several reactions are involved in the production of cumulenes (CH, C, C_2) + (C_nH, C_nH_2), and the photodissociation of the radicals C_nH. The photodissociation of the clusters into fragments C_3+C_{n-3} maintains a high abundance for triatomic carbon. The available data for C_3 indicate that this species reacts slowly with most small hydrocarbons, but very fast with large C_nH_m species. The reduction of the C_2 abundance through R12 makes C_3 the most abundant carbon species after a short evolution time in the three zones. The reaction between C_n, C_nH, and C_nH_2 (i.e., the most abundant C-rich species) will drive the growth of very small grains (VSG). The degree of hydrogenation of these large carbon clusters will depend on the rates of reactions involving C_n with either C_nH_2, C_nH, or H_2. Assuming low rates for the reaction C_n+H_2, these VSG will have C/H $\gg 1$. The C_n clusters are more abundant than polyynes for $t > 1$ yr. Whether the growth of VSG is toward amorphous carbon or toward much more structured species (fullerenes or exotic cyclic structures) will depend on the reactions between small cumulenes themselves (all their isomers). The only available data are the rates measured by Kruse & Roth (1997) at high temperature for $C_2 + C_2 = C_3 + C$ and $C_3 + C_2 = C_4 + C$ ($T > 2000$ K; $k \simeq 5 \times 10^{-10}$). If similar rates do apply at lower temperatures and if they can be generalized to $C_n + C_m = C_{n+m-k} + C_k$, then carbon clusters will grow easily. The large number of unidentified infrared absorption bands around 8 μm found in CRL 618 by Cernicharo et al (2001a, 2001b) could be due to combination bands of the bending modes of medium-size carbon clusters ($n < 15$–20). Carbon clusters are also efficiently produced for much lower densities and radiation fields, like in IRC +10216. Recently, tetraatomic carbon (C_4) has been tentatively identified in IRC +10216, CRL 618, CRL 2688, and NGC 7027, and also the interstellar medium (Cernicharo et al. 2002).

Reactions between radicals and other species, in particular CH_4 and C_2H_4, and with their photodissociation products, lead to large molecules and radicals, C_nH_3 and C_nH_4. However, because of the large H_2 volume density, only the smaller products, C_3H_3 and C_4H_4 (vinyl-acetylene), are abundant. C_4H_4 is formed

in the reaction of C_2H_4 and C_2H and reaches abundances $\simeq 10^{-5}$ in the three zones. C_3H_4 (H_2CCCH_2 or CH_3CCH) is also efficiently produced, with a peak abundance of 2×10^{-7} (Cernicharo et al. 2001a). The reaction of C_2H_4 with CN produces vinyl-cyanide (CH_2CHCN), and the models predict an abundance of 10^{-7} for this species, which has been recently detected in CRL 618 (Cernicharo et al. 2001a). The reaction of C_2H_4 with C_4H and longer radicals will produce C_6H_4 and C_nH_4. However, no data are available for these reactions. Reactions involving polyynes and radicals C_nH_3, not yet studied in the laboratory, could also contribute to the formation of bigger molecules in the PDRP and to the formation of aromatic species. However, C_3H_3, the most abundant of these species, reacts very fast with H, hence these reactions could be important in zone III, where atomic hydrogen is less abundant. The reaction $C_3H_3 + C_3H_3 = C_6H_5$ (phenyl) + H proceeds slowly at 300 K ($k = 2.2 \times 10^{-14}$), but could be an efficient way to produce aromatics at high temperatures in the PDRP. The reaction of C_4H_4 with C_2H to form C_4H_3 (isomer I-C_4H_3) and C_2H_2 through H removal has been studied and is fast. However, the removal of one H and the insertion of the C_2H group, which could efficiently produce C_6H_4 (benzyne), has not yet been studied. Although the reactions of C_2H with C_nH_4 species is certainly very fast, nothing is known about the possible products.

O-bearing species are formed in the three zones (see Fig. 1, *bottom panels*). As soon as atomic oxygen becomes available from the dissociation of CO, the reactions of O+hydrocarbons produce four main O-bearing species: H_2CO, OH, H_2O, and CO_2. The first species is formed in R28 ($k_{300} = 1.4 \times 10^{-10}$). OH is formed from several reactions of atomic oxygen with the most abundant products of the photodissociation of CH_4 and C_2H_4 (see, e.g., R29). Water vapor is formed through R31 ($k_{300} = 2.6 \times 10^{-14}$). Finally, CO_2 is produced through R30 ($k_{300} = 1.6 \times 10^{-13}$). The abundance of H_2CO shows a strong dependency with time, because of the fast photodissociation of CH_3 (R16 and R17, which could maintain a high abundance for CH_3, have rather low rates at 300 K). Hence, this species could be considered as a transient molecule during the evolution of the PDRP. However, OH, H_2O, and CO_2 persist for a long time, reaching SS abundances in 10 yr in most cases. H_2CO reaches a peak abundance of 10^{-6} in 0.1 yr in zone I and II, and in 1 yr in zone III. The peak abundance of OH and H_2O in zones I, II, and III is 10^{-7}. Only in zone III do these species reach SS with an abundance of $\simeq 10^{-7}$. CO_2 has an abundance 100 times lower than H_2O in the models. The predicted abundances for H_2CO, H_2O, and OH agree with the observations of Cernicharo et al. (1989) and Herpin & Cernicharo (2000). For higher temperatures (600–1000 K), OH, H_2O, and CO_2 reach abundances as high as 10^{-6} to 10^{-5}. Hence, it is not necessary to invoke a change in the C/O composition of CSE to explain the presence of O-bearing species in C-rich PPNs.

When the ionization front arrives at the chemically processed neutral layers, the abundance of complex carbon molecules is large, and hydrogenization could start through reactions between C_n^+, C_nH^+, $C_nH_2^+$, and H_2. A large number of important reactions has to be studied from both theoretical and experimental points of view—i.e., (C_n, C_nH)+(C_nH, C_nH_2, CH_4, C_2H_4, H, H_2)—in order to understand the chemical evolution of C-rich PDRs in which large, complex carbon-rich molecules and VSG are efficiently produced, as indicated by the observations.

I thank Spanish MCyT for funding support under grants AYA 2000-1784, ESP 2001-4516, ESP 2002-01627, and AYA 2003-02785. I also thank M. Guélin and J. R. Pardo for their comments and suggestions, and R. Rodrigo for supplying photo cross sections for several hydrocarbons.

REFERENCES

Cernicharo, J., Goiciechea, J. R., & Benilan, Y. 2002, ApJ, 580, L157
Cernicharo, J., Guélin, M., Kahane, C. 2000, A&AS, 142, 181
Cernicharo, J., Guélin, M., Peñalver, J., Martín-Pintado, J., & Mauersberger, R. 1989, A&A, 222, L1
Cernicharo, J., Heras, A., Pardo, J. R., Tielens, A. G. G. M., Guélin, M., Dartois, E., Neri, R., & Waters, L. B. F. M. 2001a, ApJ, 546, L127
Cernicharo, J., Heras, A., Tielens, A. G. G. M., Pardo, J. R., Herpin, F., Guélin, M., & Waters, L. B. F. M. 2001b, ApJ, 546, L123
Cernicharo, J., Yamamura, I., González-Alfonso, E., de Jong, T., Heras, A., Escribano, R., & Ortigoso, J. 1999, ApJ, 526, L41
Cernicharo, J., et al. 1996, A&A, 315, L201
Chastaing, D., Le Picard, S. D., Sims, I. R., & Smith, I. W. M. 2001, A&A, 365, 241
Chastaing, D., Le Picard, S. D., Sims, I. R., Smith, I. W. M., Geppert, W. D., Naulin, C., & Costes, M. 2000, Chem. Phys. Lett., 331, 170
Choi, H., Bise, R. T., Hoops, A. A., Mordaunt, D. H., & Neumark, D. M. 2000, J. Phys. Chem. A, 104, 2025
Clary, D. C., et al. 2002, J. Phys. Chem. A, 106, 5541
Haider, N., & Hussain, D. 1993, J. Chem. Soc. Faraday Trans., 89, 7
Herbst, E. 2001, Chem. Soc. Rev., 30, 168
Herbst, E., Lee, H. H., Howe, D. A., & Millar, T. J. 1994, MNRAS, 268, 335
Herpin, F., & Cernicharo, J. 2000, ApJ, 530, L129
Kaiser, R. I., Nguyen, T. L., Le, T. N., & Mebel, A. M. 2001, ApJ, 561, 858
Kiefer, J. H., Sidhu, S. S., Kern, R. D., Xie, K., Chen, H., & Harding, L. B. 1992, Combustion Sci. Technol., 82, 101
Konnov, A. A. 2000, in 28th Symp. (Int.) on Combustion, ed. N. A. Chigier (Oxford: Pergamon), 317
Kruse, T., & Roth, P. 1997, J. Phys. Chem. A, 101, 2138
Kwok, S., & Bignell, R. C. 1984, ApJ, 276, 544
Lara, L. M., Lellouch, E., López-Moreno, J. J., & Rodrigo, R. 1996, J. Geophys. Res., 113, 2
Le Teuff, Y. H., Millar, T. J., & Markwick, A. J. 1999, A&AS, 146, 157
Martin-Pintado, J., Bujarrabal, V., Bachiller, R., & Planesas, P. 1988, A&A, 197, L15
Millar, T. J., Herbst, E., & Bettens, R. P. A. 2000, MNRAS, 316 195
Moses, J. I., Bézard, B., Lellouch, E., Gladstone, G. R., Feuchtgruber, H., & Allen, M. 2000a, Icarus, 143, 244
Moses J. I., Lellouch, E., Bézard, B., Gladstone, G. R., Feuchtgruber, H., & Allen, M. 2000b, Icarus, 145, 166
Peeters, J., Ceursters, B., Nguyen, H. M. T., & Nguyen, M. T. 2002, J. Chem. Phys., 116, 3700
Pitts, W. M. L., Pasternack, L., & McDonald, J. R. 1982, Chem. Phys. 68, 417
Reisler, H., Mangir, M. S., & Wittig, C. 1980, J. Chem. Phys., 73, 2280
Toublanc, D., Parisot, J. P., Brillet, J., Gautier, D., Raulin, F., & McKay, C. P. 1995, Icarus, 113, 2
Waters, L. B. F. M., et al. 1998, Nature, 391, 868